

¹⁸F-Florbetapir PET in Patients with Frontotemporal Dementia and Alzheimer Disease

Christopher Kobylecki^{1,2}, Tobias Langheinrich^{1,2}, Rainer Hinz¹, Emma R.L.C. Vardy^{1,3,4}, Gavin Brown¹, María-Elena Martino^{1,5}, Cathleen Haense⁶, Anna M. Richardson^{2,7}, Alexander Gerhard^{1,2}, Jose M. Anton-Rodriguez¹, Julie S. Snowden^{1,2}, David Neary^{1,2}, Michael J. Pontecorvo⁸, and Karl Herholz¹

¹Institute of Brain, Behaviour and Mental Health, University of Manchester, Manchester, United Kingdom; ²Cerebral Function Unit, Greater Manchester Neurosciences Centre, Salford Royal NHS Foundation Trust, Salford, United Kingdom; ³Institute of Neuroscience and Newcastle University Institute of Ageing, Newcastle University, Newcastle upon Tyne, United Kingdom; ⁴Department of Older Peoples Medicine, Newcastle upon Tyne Hospitals NHS Foundation Trust, Newcastle upon Tyne, United Kingdom; ⁵Unidad de Medicina y Cirugía Experimental, Instituto de Investigación Sanitaria Gregorio Marañón, Madrid, Spain; ⁶Department of Nuclear Medicine, Hannover Medical School, Hannover, Germany; ⁷Manchester Medical School, University of Manchester, Manchester, United Kingdom; and ⁸Avid Radiopharmaceuticals, Philadelphia, Pennsylvania

Pathologic deposition of amyloid β (A β) protein is a key component in the pathogenesis of Alzheimer disease (AD) but not a feature of frontotemporal dementia (FTD). PET ligands for A β protein are increasingly used in diagnosis and research of dementia syndromes. Here, we report a PET study using ¹⁸F-florbetapir in healthy controls and patients with AD and FTD. **Methods:** Ten healthy controls (mean age \pm SD, 62.5 \pm 5.2 y), 10 AD patients (mean age \pm SD, 62.6 \pm 4.5), and 8 FTD patients (mean age \pm SD, 62.5 \pm 9.6) were recruited to the study. All patients underwent detailed clinical and neuropsychologic assessment and T1-weighted MR imaging and were genotyped for apolipoprotein E status. All participants underwent dynamic ¹⁸F-florbetapir PET on a high-resolution research tomograph, and FTD patients also underwent ¹⁸F-FDG PET scans. Standardized uptake value ratios (SUVRs) were extracted for pre-defined gray and white matter regions of interest using cerebellar gray matter as a reference region. Static PET images were evaluated by trained raters masked to clinical status and regional analysis. **Results:** Total cortical gray matter ¹⁸F-florbetapir uptake values were significantly higher in AD patients (median SUVR, 1.73) than FTD patients (SUVR, 1.13, $P = 0.002$) and controls (SUVR, 1.26, $P = 0.04$). ¹⁸F-Florbetapir uptake was also higher in AD patients than FTD patients and controls in the frontal, parietal, occipital, and cingulate cortices and in the central subcortical regions. Only 1 FTD patient (homozygous for apolipoprotein E ϵ 4) displayed high cortical ¹⁸F-florbetapir retention, whereas ¹⁸F-FDG PET demonstrated mesio-frontal hypometabolism consistent with the clinical diagnosis of FTD. Most visual raters classified 1 control (10%) and 8 AD (80%) and 2 FTD (25%) patients as amyloid-positive, whereas ratings were tied in another 2 FTD patients and 1 healthy control. **Conclusion:** Cortical ¹⁸F-florbetapir uptake is low in most FTD patients, providing good discrimination from AD. However, visual rating of FTD scans was challenging, with a higher rate of discordance between interpreters than in AD and control subjects.

Key Words: amyloid; PET; Alzheimer's disease; frontotemporal dementia; diagnosis

J Nucl Med 2015; 56:386–391

DOI: 10.2967/jnumed.114.147454

Frontotemporal dementia (FTD) is the second most common cause of presenile dementia (1), typically presenting with early loss of insight and behavioral change (2). However, early diagnosis may be challenging given the overlap between clinical features seen in FTD and other neurodegenerative conditions such as Alzheimer disease (AD) (3). Clinicopathologic studies suggest that 10%–20% of patients with a clinical diagnosis of FTD have AD pathology, whereas the standard clinical criteria for AD before 2011 had poor diagnostic specificity (4,5). Symptomatic therapies, such as cholinesterase inhibitors, that are effective in AD do not have proven efficacy in FTD (6). The identification of biomarkers capable of predicting underlying neuropathology is therefore a critical aim to both improve diagnostic accuracy and identify patients suitable for trials of putative symptomatic therapies and disease-modifying agents.

Regional deposition of fibrillary amyloid β (A β) protein is one of the principal pathologic substrates of AD, whereas patients with FTD exhibit a range of nonamyloid pathologic changes of frontotemporal lobar degeneration (FTLD). PET studies in patients with AD have identified increased cortical and subcortical retention of ¹¹C-labeled Pittsburgh compound B (¹¹C-PiB), which binds to fibrillary A β (7). Initial studies showed significantly lower neocortical ¹¹C-PiB retention in patients with FTD than in patients with AD, although several ¹¹C-PiB-positive FTD patients were reported (8,9). Higher white matter ¹¹C-PiB binding in AD patients than FTD patients is reported by some authors (8). In a subsequent larger diagnostic study in 45 FTLD and 62 AD patients, ¹¹C-PiB PET was shown to have 89%–90% sensitivity for AD and specificity comparable to ¹⁸F-FDG PET, with complete congruency between visual interpretation of ¹¹C-PiB images and known histopathology (10). Thus, amyloid imaging represents an important potential biomarker for the differential diagnosis of AD and FTD.

Despite the diagnostic utility of ¹¹C-PiB, its widespread use is limited by issues including limited production capacity and short half-life. ¹⁸F-Florbetapir ((*E*)-4-(2-(6-(2-(2-(¹⁸F-fluoroethoxy)ethoxy)ethoxy)pyridin-3-yl)vinyloxy)-*N*-methyl benzeneamine) is 1 of 3

Received Oct. 1, 2014; revision accepted Nov. 6, 2014.

For correspondence or reprints contact: Karl Herholz, Wolfson Molecular Imaging Centre, University of Manchester, 27 Palatine Rd., Withington, Manchester M20 3LJ.

E-mail: karl.herholz@manchester.ac.uk

Published online Feb. 5, 2015.

COPYRIGHT © 2015 by the Society of Nuclear Medicine and Molecular Imaging, Inc.

fluorine-labeled A β PET ligands developed to overcome these limitations. Cortical ¹⁸F-florbetapir uptake is higher in AD patients than controls and correlates well with amyloid and plaque burden post-mortem (11,12). However, data on ¹⁸F-florbetapir PET imaging in FTD have not hitherto been published. We hypothesized that gray matter retention of ¹⁸F-florbetapir would be increased in patients with AD, compared with those with FTD and healthy controls. As secondary objectives, we wished to quantify white matter ¹⁸F-florbetapir uptake in patients with FTD as compared with those with AD and examine the effect of apolipoprotein E (*APOE*) genotype, a risk factor for AD, on ¹⁸F-florbetapir retention in FTD (13).

MATERIALS AND METHODS

Subjects

Ten healthy controls, 10 patients with mild to moderate AD, and 8 patients with behavioral variant FTD were recruited to the study. Participants with AD met National Institute of Neurological and Communicative Disorders and Stroke and the Alzheimer's Disease and Related Disorders Association criteria for probable AD (14) and had a Mini-Mental State Examination (MMSE) score of 10–24 inclusive, whereas participants with FTD met consensus diagnostic criteria (2). All patients gave written informed consent to participate in the study, or if they lacked capacity advice was sought from a consultee under the provisions of the Mental Capacity Act 2005. The study was approved by the Newcastle and North Tyneside Research Ethics Committee (approval no. 08/H0907/158) and Administration of Radioactive Substances Advisory Committee (no. 595/3586/24024).

Participants were screened for comorbidities, and a neuropsychologic evaluation including MMSE and Clinical Dementia Rating scale was performed. Exclusion criteria included neurodegenerative disorders other than FTD and AD, clinically significant systemic disease, recent substance abuse, clinically significant electrocardiogram abnormalities or laboratory evaluations, and severe drug allergy or hypersensitivity. Genetic testing for *APOE* genotype was performed in all subjects with AD and FTD.

MR Imaging

All participants underwent structural T1-weighted MR imaging on a 3-T Achieva scanner (Philips) using an 8-element SENSE (Sensitivity ENcoding Spin Echo) head coil. A T1-weighted inversion recovery sequence was used with the following parameters: fast field echo; field of view, 256; matrix, 256 × 256; SENSE acceleration factor, 2; slice thickness, 1 mm; 150 contiguous slices; acquired voxel size, 1.0 × 1.25 × 1.0 mm reconstructed to 1.0 × 1.0 × 1.0 mm (repetition time, 8.4 ms; echo time, 3.8 ms; inversion time, 1,150 ms).

PET Imaging

All participants underwent PET imaging with ¹⁸F-florbetapir on the high-resolution research tomograph (HRRT; CTI/Siemens); in the case of FTD patients, amyloid imaging was performed at least 24 h but no more than 14 d after the ¹⁸F-FDG PET. Participants were positioned optimally within the scanner, and a 7-min transmission scan to allow for attenuation correction was obtained. Participants received a slow bolus intravenous injection of 10 mL of 288.3 ± 18.2 MBq of ¹⁸F-florbetapir over 20 s (range, 244.8–315.3; target dose, 300 MBq) 7 min after the start of the subsequent emission scan, followed by a slow bolus saline flush. PET data were acquired for a total of 60 min after injection in list-mode and were reconstructed using an ultra-fast ordered-subsets expectation maximization algorithm (15) (matrix size, 256 × 256 × 207; voxel size, 1.22 × 1.22 × 1.22 mm). Centroid of motion data were used to correct for head motion by realignment of frames as previously described (16).

All FTD patients also underwent ¹⁸F-FDG PET imaging on the HRRT to provide additional diagnostic information. Participants fasted for a minimum of 6 h before PET imaging. Participants were optimally positioned within the scanner, and a 7-min transmission scan to allow for attenuation correction was obtained. A slow bolus intravenous injection of 10 mL of 185 MBq of ¹⁸F-FDG was given over 20 s 7 min subsequent to the start of emission scan, followed by a slow bolus saline flush. PET data were acquired for a total of 60 min after injection in list-mode and reconstructed as described above.

Image Analysis

Motion-corrected summed ¹⁸F-florbetapir PET images (50–60 min) for each subject were coregistered to the structural MR images using SPM8 (Wellcome Trust Centre for Neuroimaging) running in MATLAB (r2011a; The MathWorks). The quality of coregistration was checked visually for each subject. Unified segmentation of structural T1-weighted MR images was performed in SPM8, after which a modified probabilistic anatomic atlas (17) was normalized to each individual subject's anatomic space (Supplemental Fig. 1; supplemental materials are available at <http://jnm.snmjournals.org>). Gray and white matter object maps were created by convolving the normalized anatomic atlas with binary gray and white matter masks, and uptake values were extracted in ANALYZE 10.0 (AnalyzeDirect) (18). The average of all neocortical areas was presented as the mean cortical uptake value. The borders of white matter tissue regions kept a distance of at least 4 mm from gray matter. Intensity normalization of all region-of-interest (ROI) values was performed to the mean gray matter cerebellar uptake to produce standardized uptake value ratios (SUVRs).

TABLE 1
Demographic Information on Subjects Recruited to Study

Characteristic	Healthy controls (<i>n</i> = 10)	FTD (<i>n</i> = 8)	AD (<i>n</i> = 10)
Age (y)	62.5 ± 5.1	62.5 ± 9.6	62.6 ± 4.5
Sex			
Male	4	8	7
Female	6		3
Disease duration (y)	—	4.6 ± 1.8	4.9 ± 1.7
MMSE	30	26.5 (0–30)	18.0 (10–24)
Total Clinical Dementia Rating score	0	1.0 (0.5–2.0)	1.0 (0.5–2.0)
<i>APOE</i> ε4 carriers (0/1/2 gene copies)	—	4/3/1	4/3/3

Data are mean ± SD for age and disease duration and median (with range in parentheses) in all other cases.

¹⁸F-florbetapir images smoothed by an 8-mm gaussian volume filter to reduce image noise were interpreted using a gray-scale display by 4 interpreters experienced in brain PET scanning who were masked to clinical diagnosis and regional analysis results. Interpreters had been trained according to current guidelines (Amyvid prescribing information; Eli Lilly) to recognize amyloid-positive scans by increased retention of tracer in cortical gray matter as shown by the apparent loss of contrast in gray or white matter in any 2 cortical regions or intense uptake in at least 1 cortical region.

Summed ¹⁸F-FDG PET images (20–60 min after injection) were visually rated by 2 investigators experienced in brain PET imaging and masked to clinical details. Visual analysis was supported by stereotactic surface projections of metabolic abnormalities using Neurostat (University of Washington, Seattle, WA) (19,20).

Statistical Analysis

Data analysis was performed using SPSS (version 20.0; IBM). Variables were assessed for normality using the Shapiro–Wilk test. Continuous data for the 3 groups were evaluated using 1-way ANOVA for normally distributed values and the Kruskal–Wallis test for nonnormally distributed values. Post hoc Tukey or Mann–Whitney tests with Bonferroni adjustment were applied. Continuous data for AD and FTD patients only were evaluated using the Student *t* test. Categorical data were evaluated using a χ^2 test. The effect of *APOE* ϵ 4 gene dosage on cortical ¹⁸F-florbetapir binding was assessed by analysis of covariance. A significance level of *P* less than 0.05 was used for all analyses.

RESULTS

Demographic and clinical data are shown in Table 1. There were no significant differences between the AD and FTD groups in terms of age, disease duration, or dementia severity as measured by MMSE or Clinical Dementia Rating (*P* > 0.05), although severity scores were significantly worse in AD and FTD patients than controls (*P* < 0.05). Sex distribution was unequal between groups, as the FTD patients were all men. There was no significant difference in distribution of *APOE* ϵ 4 alleles between the 2 disease groups (*P* > 0.05).

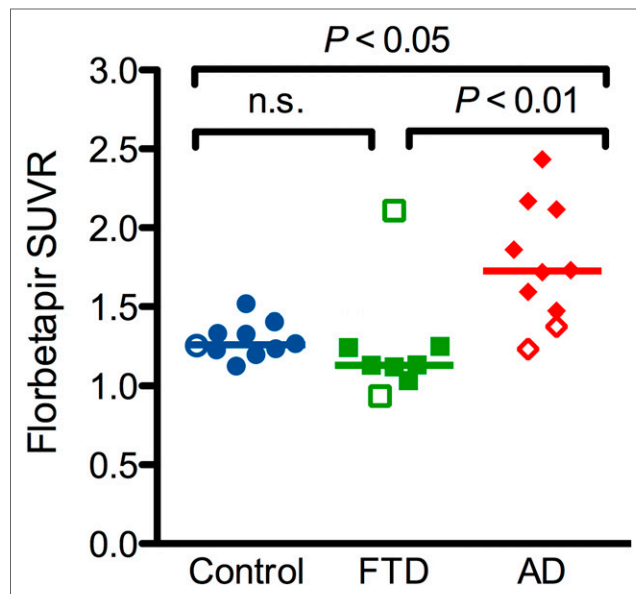


FIGURE 1. Whole neocortical ¹⁸F-florbetapir SUVRs relative to cerebellar gray matter in patients with AD and FTD and healthy controls. Points represent individual subject values and bars median values (Kruskal–Wallis test followed by pairwise post hoc test corrected for multiple comparisons). Subjects in whom most visual interpretation was discordant from their clinical diagnosis are indicated as open symbols.

Quantitative Analysis of ¹⁸F-Florbetapir PET Images

There was a significant effect of diagnostic group (Kruskal–Wallis test, *P* = 0.002) on mean cortical ¹⁸F-florbetapir binding relative to cerebellar cortex, which was lower in FTD patients (1.25 ± 0.36 ; *P* = 0.002) and controls (1.29 ± 0.11 ; *P* = 0.04) than in AD patients (1.77 ± 0.38) (Fig. 1). A threshold of 1.45 provided optimum discrimination between AD patients and controls (17/20 classified correctly), and only 1 FTD patient was above that threshold.

TABLE 2
Regional ¹⁸F-Florbetapir Uptake Ratios Normalized to Gray Matter Cerebellar Uptake for Subjects with FTD and AD and Healthy Controls

ROI	<i>P</i>	Control	FTD	AD
Mesial temporal cortex	0.014	1.08 (0.23)	0.97 (0.09)*	1.18 (0.16)
Temporal cortex	0.002	1.21 (0.17)	1.08 (0.22)†	1.54 (0.58)
Frontal cortex	0.001	1.29 (0.16)*	1.17 (0.18)†	1.85 (0.88)
Anterior cingulate cortex	0.002	1.38 (0.29)*	1.21 (0.23)†	1.91 (0.89)
Posterior cingulate cortex	0.004	1.31 (0.22)*	1.20 (0.43)†	1.94 (0.85)
Parietal cortex	0.004	1.31 (0.16)*	1.21 (0.29)†	1.85 (0.77)
Occipital cortex	0.001	1.31 (0.16)*	1.18 (0.19)†	1.67 (0.41)
Caudate nucleus	0.001	1.04 (0.13)†	1.02 (0.22)†	1.31 (0.34)
Putamen	0.001	1.31 (0.23)†	1.34 (0.19)*	2.09 (0.74)
Thalamus	0.003	1.09 (0.13)	1.03 (0.18)†	1.22 (0.17)
Brain stem	0.993	1.20 (0.16)	1.19 (0.26)	1.18 (0.21)
Whole-brain white matter	0.24	2.51 (0.63)	2.34 (0.54)	2.59 (0.55)

**P* < 0.05 vs. AD (Kruskal–Wallis test followed by post hoc pairwise tests adjusted for multiple comparisons).

†*P* < 0.01 vs. AD (Kruskal–Wallis test followed by post hoc pairwise tests adjusted for multiple comparisons).

Data are presented as median, with interquartile range in parentheses, in all cases.

¹⁸F-Florbetapir binding was significantly increased in AD subjects, compared with FTD and healthy controls in most ROIs, including posterior and anterior cingulate cortices, as well as frontal, parietal, and occipital neocortices and subcortical gray matter regions (Table 2). There was no significant difference between AD patients and controls in mesial temporal lobe structures, although ¹⁸F-florbetapir binding in this region was higher in AD than FTD. There were no significant differences in ¹⁸F-florbetapir binding in FTD, compared with controls, in any area tested. The analysis of white matter uptake ratios revealed no significant differences between groups in any ROI or overall white matter binding (Table 2).

Visual Analysis of PET Images

As shown in Supplemental Table 1, most interpreters identified 1 positive ¹⁸F-florbetapir scan of 10 healthy control subjects and 2 negative scans in 10 AD patients. In 1 control, visual ratings were tied (2 positive, 2 negative). Of the 8 FTD patients, 4 were rated by majority as amyloid-negative, 2 as positive (patients 12 and 18), and 2 were tied (patients 14 and 15). Overall, there was a moderate agreement among interpreters (Fleiss's κ , 0.57). Disagreement tended to be more frequent in patients with FTD (5/8) than in patients with AD and controls (6/20).

Only 1 of the FTD patients (patient 18) was rated positive by all interpreters and exhibited increased cortical ¹⁸F-florbetapir binding in quantitative analysis, with all cortical regions within the range seen in AD patients. This patient had presented with symptoms since the age of 64, with a history of disinhibition and a loss of empathy and judgment, and lacked insight into his problems. MMSE was 26 of 30, and neuropsychologic evaluation showed executive dysfunction, with inefficient memory secondary to this, but normal perceptuospatial function. On clinical follow-up, he remained disinhibited and inattentive and showed marked impairment on an emotion recognition task. His ¹⁸F-FDG PET scan showed marked frontotemporal hypometabolism with relative preservation of posterior cingulate/precuneus, consistent with the clinical diagnosis of FTD (Supplemental Fig. 2). Uniquely among the FTD cohort, this subject was homozygous for the *APOE* ϵ 4 allele, consistent with the positive amyloid finding.

On visual examination of ¹⁸F-FDG PET images by 2 neurologists experienced in brain PET imaging, a degree of frontal hypometabolism was seen in all FTD patients, whereas no patients displayed a pattern typical for AD. In 2 patients, changes assessed visually and by stereotactic surface projection were mild. Three patients showed pronounced anterior temporal hypometabolism in addition to the frontal changes. Four patients also showed some degree of parietal or occipital hypometabolism, whereas no patients had bilateral metabolic impairment of the posterior cingulate or precuneus.

DISCUSSION

We report the first study, to our knowledge, of ¹⁸F-florbetapir PET imaging in patients with FTD, compared with those with AD. Consistent with previous studies, neocortical and subcortical gray matter ¹⁸F-florbetapir retention was increased in patients with AD, compared with healthy controls (21,22). In line with the primary study hypothesis, ¹⁸F-florbetapir binding was significantly increased in the cortical and subcortical gray matter of patients with AD relative to those with FTD.

The visual interpretation data in our study with respect to AD patients and controls were comparable to those reported in previous studies (21,22) and in line with the overlap seen on regional analysis (Fig. 1) between patients with AD and healthy controls. However, rating FTD patients was challenging, with only

2 of 8 FTD scans unanimously rated as negative, and the high disagreement rate indicated considerable uncertainty, whereas quantitative regional analysis identified increased global cortical binding comparable to AD in only 1 FTD patient. Retrospective unmasked inspection of scans in conjunction with MR scans revealed that severe cortical atrophy had confounded visual rating of some scans by mimicking high cortical uptake in some brain areas (Fig. 2B). Two FTD patients (patients 12 and 15) and 1 control subject (subject 22), who had received positive ratings, also had low cerebral white matter SUVR (1.91, 1.84, and 1.86, respectively, compared with a median of 2.46; interquartile range, 1.98–2.72, in entire sample). This low cerebral white matter may have reduced the contrast between gray and white matter that was guiding visual interpretation. Scans with discordant ratings did not show the typical full AD pattern but had reduced gray/white matter contrast in some lobes to a degree that fulfilled formal criteria for scan positivity (Fig. 3). Possible reasons of that appearance included regional cortical atrophy, low tracer uptake in white matter, and minor head movement. As demonstrated in Figure 3, MR image coregistration and image fusion could have clarified the actual gray/white matter borders, demonstrating the actual contrast and thus, perhaps, preventing misclassification. This somewhat atypical appearance contrasts with the unequivocally increased cortical ¹⁸F-florbetapir uptake seen in subjects with elevated ¹⁸F-florbetapir SUVRs (Figs. 2A and 2C). These observations suggest that visual interpretation of ¹⁸F-florbetapir images may be challenging

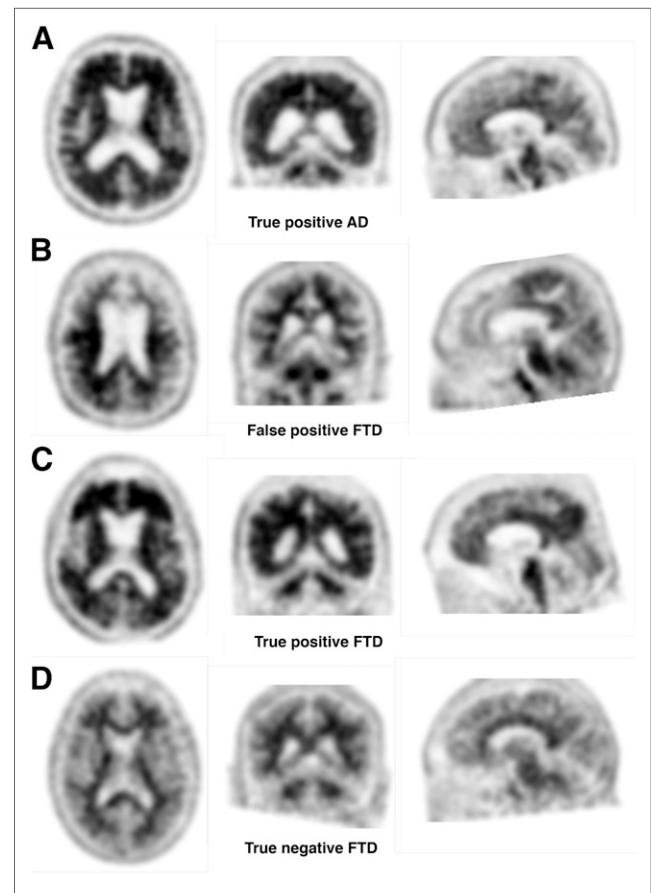


FIGURE 2. Gray-scale ¹⁸F-florbetapir scans as used for visual interpretation. (A) Patient 4 in Supplemental Table 1, patient 12 (B), patient 18 (C), patient 11 (D).

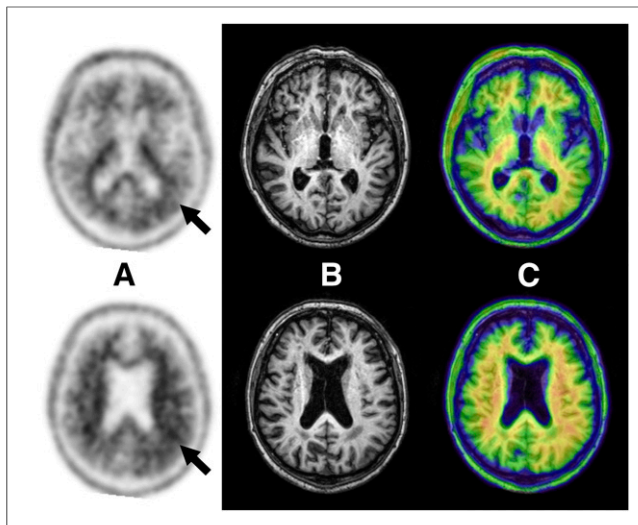


FIGURE 3. Transaxial coregistered images from FTD subject with discordant visual interpretations (subject 15 in Supplemental Table 1) of gray-scale ^{18}F -florbetapir PET (A), T1-weighted MR brain (B), and color-scale ^{18}F -florbetapir PET fused to MR brain (C). Arrows indicate apparent areas of high ^{18}F -florbetapir uptake as a result of loss of contrast due to low white matter uptake or cortical atrophy leading to inconsistent visual interpretations.

in patients with FTD, and guidance should be refined on the basis of further studies in FTD using standard clinical scanners.

Limitations of our study include the relatively small sample size and the use of clinical diagnosis as a standard of truth, in the absence of pathologic verification. However, clinical diagnosis was based on the assessment of experienced clinicians working in a tertiary cognitive neurology unit with a good record for diagnostic accuracy in AD and FTLD as confirmed by clinicopathologic studies (23). In addition, none of the FTD patients had patterns of ^{18}F -FDG hypometabolism typical for AD. However, as only FTD patients underwent ^{18}F -FDG PET, the diagnostic utility of ^{18}F -florbetapir, compared with ^{18}F -FDG PET, cannot be estimated. Given that our FTD cohort met research criteria for FTD, the generalizability of our findings to clinical situations in which there is a genuine diagnostic equipoise between AD and FTD is potentially limited. Previous ^{11}C -PiB data from patients with pathologically confirmed FTLD showed that all were visually rated as negative for amyloid (10). A strength of our study is that study groups were well matched in terms of age, relatively short disease duration, and dementia severity. Although the groups were not balanced in terms of sex, previous data suggest that PiB binding is greater in men with AD (24), and therefore the greater proportion of men in the FTD group in this study is unlikely to have influenced the outcome.

Our findings in FTD are consistent with other published studies using ^{11}C -PiB, in which lower neocortical uptake has been observed relative to AD (8–10). We used a different method to delineate ROIs for our analysis, namely an atlas-based approach after segmentation of anatomic MR imaging scans, in contrast to previous papers (8,9). Together with motion correction of the PET data, MR-based segmentation should improve the accuracy of ROI definition and minimize the effect of spill-over from adjacent regions. Although we did not perform partial-volume correction on these data, this is comparable to existing studies reporting amyloid imaging in FTD, including a recent report of another ^{18}F -labeled tracer, florbetaben (25). Studies on partial-volume correction of ^{11}C -PiB data suggest that our approach may underestimate

group differences between AD and other conditions, so the absence of partial-volume correction is unlikely to invalidate our findings (26). In most previous studies, ^{18}F -florbetapir SUVRs were calculated with reference to the entire cerebellum (21,22). We used the cerebellar cortex to avoid contamination of the reference values by the variation of nonspecific cerebellar white matter uptake, whereas SUVRs calculated with either method were highly correlated ($R^2 = 0.89$).

Previous studies have suggested a significant overlap between AD and FTD patients in binding of ^{11}C -PiB, with 2–4 positive subjects in cohorts of a size comparable to that reported here (8,9). However, several of these reported cases had neuropsychologic features, a subsequent clinical course, or ^{18}F -FDG PET findings to suggest an alternative diagnosis of AD (8,9). Patients with pathologically confirmed AD may have behavioral features of FTD at presentation, although they tend to develop neuropsychologic features, such as visuospatial impairment, characteristic of AD during the disease course (4,27). However, the clinical features, subsequent clinical course, and ^{18}F -FDG imaging of the FTD patients with high regional uptake were all in keeping with the clinical diagnosis of FTD. One FTD patient was homozygous for the *APOE* $\epsilon 4$ allele and showed elevated neocortical ^{18}F -florbetapir retention, in line with previous studies demonstrating that *APOE* $\epsilon 4$ is associated with higher amyloid burden (13). Deposition of $\text{A}\beta$ has also been described in pathologically confirmed FTLD (28), with a greater $\text{A}\beta$ burden in *APOE* $\epsilon 4$ carriers and extensive neuritic plaque deposition in an *APOE* $\epsilon 4$ homozygote. A positive ^{18}F -florbetapir PET scan has also been reported recently in a patient with frequent cortical neuritic plaques and frontotemporal lobar degeneration with TDP43-positive inclusions (29). Most likely, this positive scan represents FTD–AD comorbidity, with the FTD component dominating the clinical presentation.

Previous studies on the topography of white matter binding of amyloid tracers have produced variable findings. Several ^{11}C -PiB PET studies showed no significant differences in binding to subcortical white matter between AD and controls, whereas PiB did not show specific binding to white matter homogenates or post-mortem specimens from AD patients (7,30). Other studies have reported elevated ^{11}C -PiB retention in the subcortical white matter of patients with AD, compared with FTD (8), indicating the importance of resolving this issue. It is possible that white matter pathology, seen prominently in some molecular subtypes of FTD, might lead to a reduction in amyloid binding, compared with AD. When using eroded white matter masks to minimize the possibility of contamination of adjacent white matter regions by the differences in specific gray matter binding between AD and FTD due to partial-volume effects, we could not find significant differences in white matter binding between groups, whereas there was considerable interindividual variation.

Our observations underline that referring physicians should evaluate amyloid PET scan results in the context of clinical findings. Moreover, it may be useful for interpreters to indicate when the presentation is atypical and classification is uncertain. In our series, we would not have changed the clinical diagnosis in any of the FTD patients, but the scans made us aware of additional amyloid pathology in at least one of them.

CONCLUSION

This study demonstrates the discrimination of patients with AD from those with FTD and healthy controls based on high-resolution

¹⁸F-florbetapir PET scans and MR imaging-guided regional analysis. However, factors such as atrophy and relatively low white matter uptake may complicate visual interpretation of ¹⁸F-florbetapir scans in some patients with FTD, and further larger studies using standard clinical scanners are required for clarification.

DISCLOSURE

The costs of publication of this article were defrayed in part by the payment of page charges. Therefore, and solely to indicate this fact, this article is hereby marked “advertisement” in accordance with 18 USC section 1734. The study was funded by a grant from Avid radiopharmaceuticals, Alzheimer Research U.K., and NIH Clinical Lectureships. No other potential conflict of interest relevant to this article was reported.

ACKNOWLEDGMENTS

We are grateful to Dr. Anupa Arora and Dr. Raj Agarwal for interpreting scans.

REFERENCES

1. Ratnavalli E, Brayne C, Dawson K, Hodges JR. The prevalence of frontotemporal dementia. *Neurology*. 2002;58:1615–1621.
2. Neary D, Snowden JS, Gustafson L, et al. Frontotemporal lobar degeneration: a consensus on clinical diagnostic criteria. *Neurology*. 1998;51:1546–1554.
3. Galton CJ, Patterson K, Xuereb JH, Hodges JR. Atypical and typical presentations of Alzheimer’s disease: a clinical, neuropsychological, neuroimaging and pathological study of 13 cases. *Brain*. 2000;123:484–498.
4. Forman MS, Farmer J, Johnson JK, et al. Frontotemporal dementia: clinicopathological correlations. *Ann Neurol*. 2006;59:952–962.
5. Varma AR, Snowden JS, Lloyd JJ, Talbot PR, Mann DM, Neary D. Evaluation of the NINCDS-ADRDA criteria in the differentiation of Alzheimer’s disease and frontotemporal dementia. *J Neurol Neurosurg Psychiatry*. 1999;66:184–188.
6. Seltman RE, Matthews BR. Frontotemporal lobar degeneration: epidemiology, pathology, diagnosis and management. *CNS Drugs*. 2012;26:841–870.
7. Klunk WE, Engler H, Nordberg A, et al. Imaging brain amyloid in Alzheimer’s disease with Pittsburgh compound-B. *Ann Neurol*. 2004;55:306–319.
8. Rabinovici GD, Furst AJ, O’Neil JP, et al. ¹¹C-PIB PET imaging in Alzheimer disease and frontotemporal lobar degeneration. *Neurology*. 2007;68:1205–1212.
9. Engler H, Santillo AF, Wang SX, et al. In vivo amyloid imaging with PET in frontotemporal dementia. *Eur J Nucl Med Mol Imaging*. 2008;35:100–106.
10. Rabinovici GD, Rosen HJ, Alkalay A, et al. Amyloid vs FDG-PET in the differential diagnosis of AD and FTLD. *Neurology*. 2011;77:2034–2042.
11. Wong DF, Rosenberg PB, Zhou Y, et al. In vivo imaging of amyloid deposition in Alzheimer disease using the radioligand ¹⁸F-AV-45 (florbetapir [corrected] F 18). *J Nucl Med*. 2010;51:913–920.
12. Clark CM, Schneider JA, Bedell BJ, et al. Use of florbetapir-PET for imaging beta-amyloid pathology. *JAMA*. 2011;305:275–283.
13. Fleisher AS, Chen K, Liu X, et al. Apolipoprotein E epsilon4 and age effects on florbetapir positron emission tomography in healthy aging and Alzheimer disease. *Neurobiol Aging*. 2013;34:1–12.
14. McKhann G, Drachman D, Folstein M, Katzman R, Price D, Stadlan EM. Clinical diagnosis of Alzheimer’s disease: report of the NINCDS-ADRDA Work Group under the auspices of Department of Health and Human Services Task Force on Alzheimer’s Disease. *Neurology*. 1984;34:939–944.
15. Segobin S, Matthews J, Coope D, et al. Motion detection from raw list-mode HRRT data and improved frame-by-frame realignment for motion correction [abstract]. *J Nucl Med*. 2009;50:589.
16. Hong IK, Chung ST, Kim HK, Kim YB, Son YD, Cho ZH. Ultra fast symmetry and SIMD-based projection-backprojection (SSP) algorithm for 3-D PET image reconstruction. *IEEE Trans Med Imaging*. 2007;26:789–803.
17. Hammers A, Allom R, Koepp MJ, et al. Three-dimensional maximum probability atlas of the human brain, with particular reference to the temporal lobe. *Hum Brain Mapp*. 2003;19:224–247.
18. Robb RA, Hanson DP. A software system for interactive and quantitative visualization of multidimensional biomedical images. *Australas Phys Eng Sci Med*. 1991;14:9–30.
19. Ishii K, Willoch F, Minoshima S, et al. Statistical brain mapping of ¹⁸F-FDG PET in Alzheimer’s disease: validation of anatomic standardization for atrophied brains. *J Nucl Med*. 2001;42:548–557.
20. Minoshima S, Frey KA, Koeppe RA, Foster NL, Kuhl DE. A diagnostic approach in Alzheimer’s disease using three-dimensional stereotactic surface projections of fluorine-18-FDG PET. *J Nucl Med*. 1995;36:1238–1248.
21. Fleisher AS, Chen K, Liu X, et al. Using positron emission tomography and florbetapir F18 to image cortical amyloid in patients with mild cognitive impairment or dementia due to Alzheimer disease. *Arch Neurol*. 2011;68:1404–1411.
22. Johnson KA, Sperling RA, Gidicsin CM, et al. Florbetapir (F18-AV-45) PET to assess amyloid burden in Alzheimer’s disease dementia, mild cognitive impairment, and normal aging. *Alzheimers Dement*. 2013;9(5, suppl):S72–S83.
23. Snowden JS, Thompson JC, Stopford CL, et al. The clinical diagnosis of early-onset dementias: diagnostic accuracy and clinicopathological relationships. *Brain*. 2011;134:2478–2492.
24. Rowe CC, Ellis KA, Rimajova M, et al. Amyloid imaging results from the Australian Imaging, Biomarkers and Lifestyle (AIBL) study of aging. *Neurobiol Aging*. 2010;31:1275–1283.
25. Villemagne VL, Ong K, Mulligan RS, et al. Amyloid imaging with ¹⁸F-florbetapir in Alzheimer disease and other dementias. *J Nucl Med*. 2011;52:1210–1217.
26. Thomas BA, Erlandsson K, Modat M, et al. The importance of appropriate partial volume correction for PET quantification in Alzheimer’s disease. *Eur J Nucl Med Mol Imaging*. 2011;38:1104–1119.
27. Alladi S, Xuereb J, Bak T, et al. Focal cortical presentations of Alzheimer’s disease. *Brain*. 2007;130:2636–2645.
28. Mann DM, McDonagh AM, Pickering-Brown SM, Kowa H, Iwatsubo T. Amyloid beta protein deposition in patients with frontotemporal lobar degeneration: relationship to age and apolipoprotein E genotype. *Neurosci Lett*. 2001;304:161–164.
29. Serrano GE, Sabbagh MN, Sue LI, et al. Positive florbetapir PET amyloid imaging in a subject with frequent cortical neuritic plaques and frontotemporal lobar degeneration with TDP43-positive inclusions. *J Alzheimers Dis*. 2014;42:813–821.
30. Fodero-Tavoletti MT, Rowe CC, McLean CA, et al. Characterization of PiB binding to white matter in Alzheimer disease and other dementias. *J Nucl Med*. 2009;50:198–204.